Vol 18 No 11, November 2009
1674-1056/2009/18(11)/4834-06

Chinese Physics B

© 2009 Chin. Phys. Soc.
and IOP Publishing Ltd

Interference of dissociating wave packets in the I_2 molecule driven by femtosecond laser pulses*

Han Yong-Chang(韩永昌), Hu Wen-Hui(胡文辉),
Yu Jie(于 杰), and Cong Shu-Lin(丛书林)†
Department of Physics, Dalian University of Technology, Dalian 116024, *China*

(Received 13 August 2008; revised manuscript received 2 March 2009)

The interference between two dissociating wave packets of the I_2 molecule driven by femtosecond laser pulses is theoretically studied by using the time-dependent quantum wave packet method. Both the internuclear distance- and velocity-dependent density functions are calculated and discussed. It is demonstrated that the interference pattern is determined by the phase difference and the delay time between two pump pulses. With two identical pulses with a delay time of 305 fs and a FWHM of 20 fs, more interference fringes can be observed, while with two pump pulses with a delay time of 80 fs and a FWHM of 20 fs, only a few interference fringes can be observed.

Keywords: photodissociation, interference of wave packets, I_2 molecule
PACC: 3390, 8250F, 8240J

1. Introduction

With the rapid development of ultrashort and ultrastrong laser pulse technology, the laser control of atomic or molecular dynamics has attracted a great deal of interest from researchers.[1,2] Many interesting phenomena have been observed and studied.[3−10] Most of them can be described by using the time-dependent wave packet method.

The wave packet interferences in bound states of an atomic or molecular system have been widely studied during the last decade. Scherer *et al* [11] reported the time-resolved fluorescence spectroscopy of interfering wave packets in a bound excited state of the I_2 molecule. They demonstrated that constructive and destructive interferences can be detected from the fluorescence by controlling the time delay and the relative phase between two laser pulses. Blanchet *et al* [12] studied the interfering wave packets in the photoionization of Cs_2. They pointed out that the ionization probability is related to the interference of wave packets and can be controlled by adjusting the laser parameters. Cina[13] developed a theoretical model used for describing wave packet interferometry. He and Humble demonstrated that time- and phase-resolved nonlinear wave packet interferometry can be used to study the molecular reconstruction.[14] Recently, molecular wave packet interferometry with high spatiotemporal resolution was studied experimentally by Ohmori *et al*.[15,16] Based on wave packet interference, various schemes have been devised to prepare special quantum states, detect wave packets and control the angular momentum of Rydberg atoms.

Unlike the wave packet interference in a bound atomic or molecular system, the wave packet interference in a free electron or dissociating molecule system provides new scope for research. The interferences of electronic wave packets have been investigated experimentally with femtosecond laser pulses,[17] few-cycle pulses[18] and soft-x-ray pulses.[19]. Based on the ion imaging technique, Skovsen *et al* [20] and Petersen *et al* [21] demonstrated that with two identical 110 fs optical pulses separated by 310 fs, the interference patterns of dissociating wave packets of the I_2 molecule can be observed. The interference patterns of the internuclear density function and the internuclear velocity density function can be measured at large internuclear distances ($R > 10$ Å). In our recent work, we demonstrated that the branching ratio of products in the photodissociation of the Br_2 molecule can be controlled by utilizing wave packet interference.[22] In the present work, we study theoretically the dissociation dynamics of the I_2 molecule driven by femtosecond laser pulses. The relationships between interference patterns and the laser parameters are studied based on the calculation of 2-dimension wave packet dynamics.

*Project supported by the National Natural Science Foundation of China (Grant Nos 10674022 and 20633070).
†Corresponding author. E-mail: shlcong@dlut.edu.cn

2. Theoretical treatments

The relevant potential energy curves (PECs)[23,24] and the transition pathways of the I_2 molecule are depicted in Fig.1. For convenience, we refer to $X^1\Sigma_g^+$ and $B^3\Pi_u^+$ as X and B, respectively. Two time-delayed pump pulses excite the I_2 molecule from the ground X state to the dissociation continuum of the B state. The two dissociating wave packets evolve on the B state, and then overlap and interfere. In the Born–Oppenheimer approximation, the wavefunctions $\boldsymbol{\Psi}(R)$ are obtained by solving the time-dependent Schrödinger equation

$$\mathrm{i}\hbar\frac{\partial}{\partial t}\boldsymbol{\Psi}(R,t) = (\hat{\boldsymbol{H}}_0 + \hat{\boldsymbol{H}}_1)\boldsymbol{\Psi}(R,t), \tag{1}$$

where $\hat{\boldsymbol{H}}_0$ is the molecular Hamiltonian in the absence of laser fields, and $\hat{\boldsymbol{H}}_1$ the field–molecule interaction.

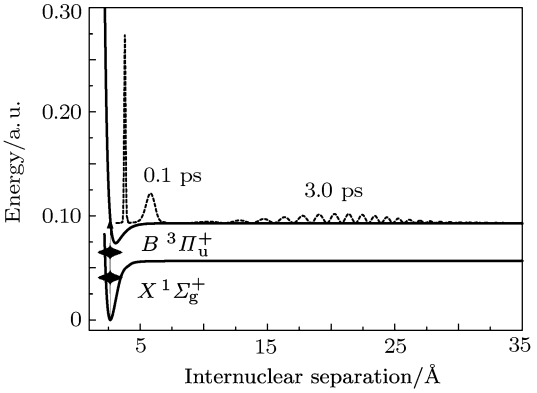


Fig.1. The potential energy curves and the transition pathways of the I_2 molecule.

In the present work, a linearly polarized laser field is used and hence the magnetic quantum number M of the molecule is conserved. We assume the initial $M = 0$, which is equivalent to ignoring the $\partial\varphi$ term (φ azimuthal angle) in a full three-dimension Hamiltonian.[25,26] The molecule is described by the azimuthally symmetric molecular Hamiltonian

$$\begin{aligned}\hat{\boldsymbol{H}}_0(R,\theta) &= \hat{\boldsymbol{T}}_R + \hat{\boldsymbol{T}}_\theta + \hat{\boldsymbol{V}}(R)\\ &= \left[-\frac{\hbar^2}{2m}\frac{\partial^2}{\partial R^2} - \frac{\hbar^2}{2mR^2}\frac{1}{\sin\theta}\frac{\partial}{\partial\theta}(\sin\theta\frac{\partial}{\partial\theta})\right]\hat{\boldsymbol{I}}\\ &\quad + \hat{\boldsymbol{V}}(R),\end{aligned} \tag{2}$$

with the volume element $\mathrm{d}\Omega = \sin\theta\mathrm{d}R\mathrm{d}\theta$, where m is the reduced mass, R is the internuclear distance and $\hat{\boldsymbol{I}}$ denotes a unit matrix. θ is the angle between the laser electric field direction and the molecular axis. $\hat{\boldsymbol{V}}(R)$ denotes the molecular potential matrix. The field–molecule interaction is given by

$$\hat{\boldsymbol{H}}_1(R,\theta,t) = \begin{pmatrix} 0 & -\mu(R)\varepsilon(t)\cos\theta \\ -\mu(R)\varepsilon(t)\cos\theta & 0 \end{pmatrix}, \tag{3}$$

where $\mu(R)$ is the transition dipole moment between two electronic states. The laser field $\varepsilon(t)$ is given by

$$\begin{aligned}\varepsilon(t) &= \varepsilon_1(t) + \varepsilon_2(t)\\ &= \varepsilon_0 f(t-t_{01})\cos[\omega_0(t-t_{01})]\\ &\quad + \varepsilon_0 f(t-t_{02})\cos[\omega_0(t-t_{02}) + \delta],\end{aligned} \tag{4}$$

with the Gaussian pulse envelope

$$f(t) = \exp\left[-4\ln 2\left(\frac{t}{T}\right)^2\right], \tag{5}$$

where T is the full width at half maximum (FWHM) of the laser pulse. In Eq.(4), ω_0 specifies the central frequency and ε_0 is the laser field amplitude. δ and $\tau = t_{02} - t_{01}$ denote the phase difference and the delay time between two pump pulses, respectively.

The initial wavefunction is taken to be the eigenfunction of the lowest rovibrational level ($|\nu = 0, j = 0\rangle$) of the X state. The rovibrational eigenfunction $|\nu, j\rangle$ is a direct product of $P_j(\xi)$ and $\phi_{\nu j}(R)$. The Legendre polynomial, $P_j(\xi)$, is the eigenfunction of the angular kinetic energy operator:

$$\hat{T}_\theta P_j(\xi) = \frac{j(j+1)\hbar^2}{2mR^2}P_j(\xi), \quad \xi = \cos\theta. \tag{6}$$

$\phi_{\nu j}(R)$ is a j-dependent radial vibrational function which can be obtained by solving numerically the following radial Schrödinger equation using the Fourier grid Hamiltonian method,[27,28]

$$\begin{aligned}&\left[-\frac{\hbar^2}{2m}\frac{\partial^2}{\partial R^2} + \frac{j(j+1)\hbar^2}{2mR^2} + V_X(R)\right]\phi_{\nu j}(R)\\ &= \epsilon_{\nu j}\phi_{\nu j}(R),\end{aligned} \tag{7}$$

where $\epsilon_{\nu j}$ is the eigenenergy of the $|\nu, j\rangle$ state. The time propagation is accomplished by using the split operator method with the short-time propagator[29]

$$\begin{aligned}\hat{U}(\Delta t) \approx\ & \mathrm{e}^{-\frac{\mathrm{i}}{2\hbar}\Delta t\hat{T}_R}\,\mathrm{e}^{-\frac{\mathrm{i}}{2\hbar}\Delta t\hat{T}_\theta}\,\mathrm{e}^{-\frac{\mathrm{i}}{\hbar}\Delta t(\hat{V}+\hat{H}_1)}\\ &\times \mathrm{e}^{-\frac{\mathrm{i}}{2\hbar}\Delta t\hat{T}_\theta}\,\mathrm{e}^{-\frac{\mathrm{i}}{2\hbar}\Delta t\hat{T}_R},\end{aligned} \tag{8}$$

where Δt is a short time step. To avoid the unphysical reflection of the wave packets at the edge, in each time step, the wavefunctions are multiplied by an absorption function,

$$V_{\rm abs}(R) = \{1 + \exp[b(R - R_{\rm abs})]\}^{-1}, \qquad (9)$$

where the parameters $R_{\rm abs}$ and b should be appropriately chosen to ensure that the wavefunction can be absorbed at large internuclear distances. In the calculation we set $R_{\rm abs} = 55.0$ Å and $b = 1.0$ Bohr^{-1}.

The internuclear distance- and velocity-dependent density functions at time t are calculated by

$$|\Psi_R(R,t)|^2 = \int |\Psi_R(R,\xi,t)|^2 {\rm d}\xi,$$
$$|\Psi_v(v,t)|^2 = \int |\Psi_v(v,\xi,t)|^2 {\rm d}\xi, \qquad (10)$$

where $\Psi_v(v,\xi,t)$ is the velocity-dependent wavefunction and is calculated by using the Flourier transform of the R-dependent wavefunction $\Psi_R(R,\xi,t)$. The velocity-dependent density function $|\Psi_v(v,t)|^2$ in the flat part of the B state is determined by laser pulses.[21,22] $\varepsilon(t)$ in the time domain can be transformed to $\widetilde{\varepsilon}(\omega)$ in the energy domain:

$$\widetilde{\varepsilon}(\omega) \propto \exp\left[-\frac{T^2(\omega-\omega_0)^2}{16\ln 2}\right] T[\cos(\omega t_{01}) + \cos(\omega t_{02} - \delta)]. \qquad (11)$$

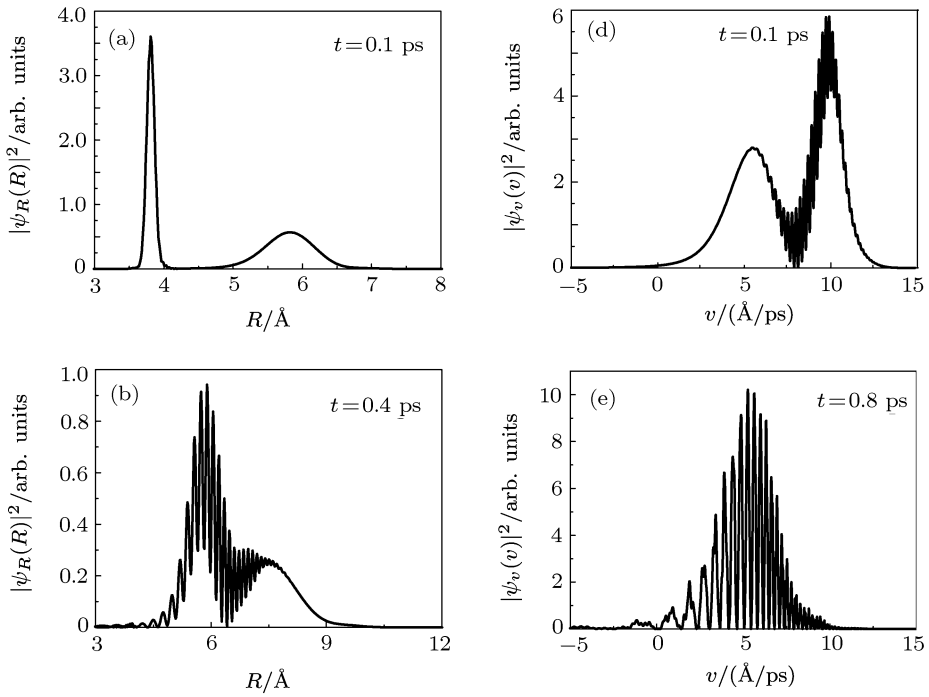
$\widetilde{\varepsilon}(\omega)$ presents the two-pump pulse spectrum. Defining the delay time as $\tau = t_{02} - t_{01}$, Eq.(11) can be written as

$$\widetilde{\varepsilon}(\omega) \propto \exp\left[-\frac{T^2(\omega-\omega_0)^2}{16\ln 2}\right] T[1 + \cos(\omega\tau - \delta)]. \qquad (12)$$

$\widetilde{\varepsilon}(\omega)$ is related to the phase difference δ, the delay time τ and the FWHM T of the two pump pulses.

3. Results and discussions

The laser-driven time-dependent Schrödinger equation (1) has been numerically solved for different laser parameters. Two pump pulses with a delay time of 305 fs are utilized to create two dissociating wave packets in the B state of the I_2 molecule. The internuclear distance-dependent density functions of the B state at $t = 0.1, 0.4$ and 5.0 ps are shown in Figs.2(a)–2(c), respectively. In Fig.2, the laser pulses are 460 nm with intensities 1.5 TW·cm^{-2} and FWHMs 20 fs. The central times of two pump pulses are $t_{01} = -305$ fs and $t_{02} = 0$, respectively. The phase difference δ between the two pump pulses is taken as zero. At $t = 0.1$ ps, as shown in Fig.2(a), the second pulse is switched off and the second wave packet is just created. Hence, the two wave packets are clearly separated at 0.1 ps. When the two wave packets propagate towards the large internuclear distance, they will spread and overlap. As shown in Fig.2(b), the second wave packet overlaps with part of the first wave packet, and an interference pattern appears. At $t = 5.0$ ps, the interference fringes of the two wave packets clearly emerge in a large region of internuclear distance, as shown in Fig.2(c).



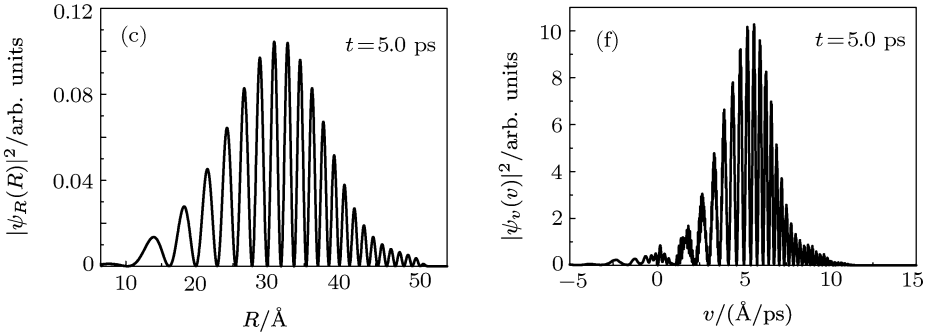


Fig.2. Snapshots of internuclear distance (R)- and velocity (v)-dependent density functions of the B state. The wavelengths of two laser pulses are 460 nm with intensities 1.5 TW·cm^{-2} and FWHMs 20 fs. The central times of two laser pulses $t_{01} = -305$ fs and $t_{02} = 0$, respectively, and the phase difference $\delta = 0$.

The internuclear velocity-dependent density functions at $t = 0.1, 0.8$ and 5.0 ps are shown in Figs.2(d)–2(f), respectively. In the Condon approximation, the wave packet is formed in the B state at about 2.6 Å which is the equilibrium internuclear distance of the X state. The dissociating wave packet is initially located in the inner potential well of the B state. It will quickly move towards the equilibrium internuclear distance of the B state and then its velocity decreases. When it arrives in the flat region of the B state, its velocity maintains an invariable value. As a result, the interference pattern of the velocity density function is not completely formed at $t = 0.1$ ps when the two wave packets lie in the well of the B state. After the two wave packets arrive in the flat region of the B state, the interference fringes display a similar pattern, as shown in Figs.2(e) and 2(f). The velocities of the two wave packets are finally centred at about 5 Å/ps. With the evolution of the wave packets, the peaks of the R-dependent density function grow broader due to the dispersion of the wave packets, while those of the velocity-dependent density function are almost invariable because the wave packet evolves in the same velocity in the flat region of the B state.

In order to study the effect of the phase difference on the interference patterns, we calculate the internuclear distance- and velocity-dependent density functions at $\delta = 0, 90°$ and 180°, respectively. Apart from the phase difference δ, the other pulse parameters are the same as those used in Fig.2. With the increase of δ, as shown in Fig.3(a), the peaks of the fringes shift in the direction of large internuclear distance. It can be expected that the fringes at $\delta = 360°$ will be the same as those at $\delta = 0$. A similar pattern is found in the velocity-dependent density function, as shown in Fig.3(b).

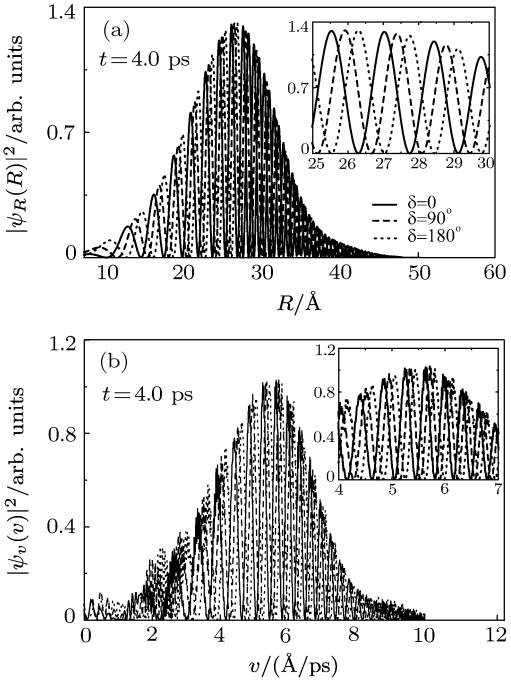


Fig.3. (a) The internuclear distance- and (b) velocity-dependent density functions at $\delta = 0, 90°$ and 180°. The laser parameters are the same as those used in Fig.2, except the phase difference δ.

In Fig.4, we illustrate the distributions of the R-dependent density functions at different delay times. The laser parameters are the same as those used in Fig.2, except the delay time τ =305, 305.5 and 306 fs. We can find from Fig.4 that when the delay time τ increases, in contrast with that in Fig.3(a),

the peaks of the fringes shift towards the small internuclear distance. From Eq.(4) we can see that $-\omega_0 t_{01(02)}$ can be treated as the phase factor of the first (second) pulse, and hence the 'phase' difference is $-\omega_0\tau$. Thus when the two different delay times satisfy $\omega_0\tau_1 - \omega_0\tau_2 = n2\pi, n = 0, 1, 2, \ldots$, the corresponding interference patterns are nearly the same. We then set $t_{02} = 0$, and change step by step the central time t_{01} of the first pulse from -305 to -307 fs in steps of 0.02 fs. We find that the interference at $\tau = 306.64$ fs displays the same pattern as that at $\tau = 305$ fs. The time difference between the two delay times is about 1.64 fs, which is just equal to the optical period at 460 nm.

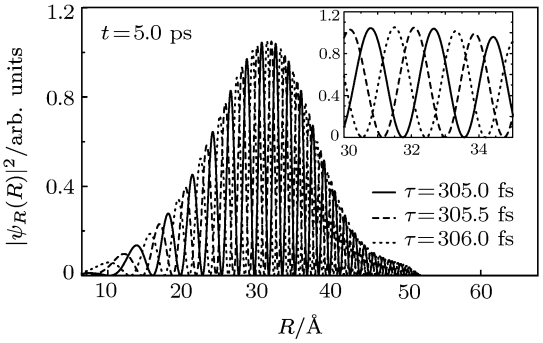


Fig.4. The internuclear distance-dependent density functions at different delay times. The laser parameters are the same as those in Fig.2, except the delay time τ.

Another kind of interference pattern emerges, when τ is equal to a relatively smaller value. The pulse parameters are taken as $t_{01} = -80$ fs and $t_{02} = 0$. The laser intensities, wavelengths and FWHMs are the same as those used in Fig.2. When τ decreases, as shown in Fig.5, the number of interference fringes decreases. Three peaks can be observed in the distributions of the R- and v-dependent density functions at 4.0 ps. From Eq.(14), we see that τ can be treated as the frequency parameter. That is to say, the number of the interference fringes will be in proportion to the parameter τ. Thus, when the delay time is large, more interference fringes can be observed; when the delay time is small, fewer interference fringes can be observed.

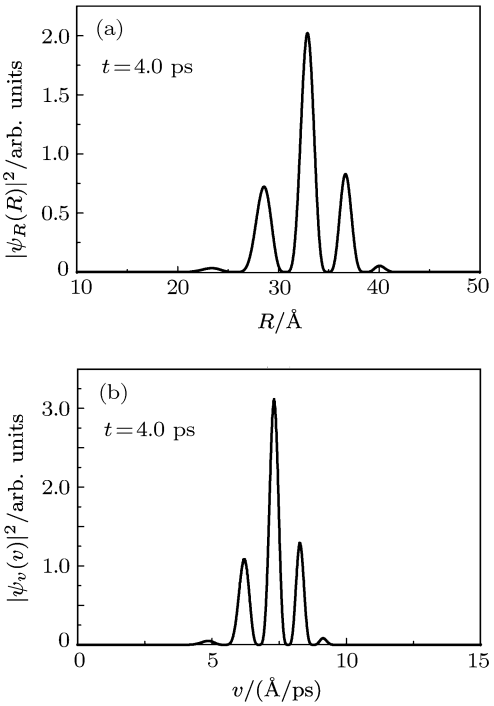


Fig.5. The R- and v-dependent density functions at $t = 4.0$ ps. The pulses parameter are chosen as follows, $T = 20$ fs, $t_{01} = -80$ fs, $t_{02} = 0$, $I = 1.5$ TW $\cdot$ cm^{-2} and the wavelengths are 460 nm.

4. Conclusions

In this paper, the interference between two dissociating wave packets in the I_2 molecule driven by femtosecond laser pulses is studied by using the 2-dimension wave packet dynamics method. It is found that the number of interference fringes is related to the delay time. With two identical pump pulses with a delay time of 305 fs and a FWHM of 20 fs, many interference fringes can be observed. However, with two pump pulses with a delay time of 80 fs and a FWHM of 20 fs, only a few interference fringes can be seen. The phase difference between the two pulses can affect the interference pattern to varying degrees. In order to obtain steady-going interference fringes, the two factors, the delay time and the phase difference, should be precisely controlled.

References

[1] Bandrauk A D 1994 *Molecules in Laser Fields* (New York: Marcel Dekker Inc.) p10

[2] Rice S A and Zhao M 2000 *Optical Control of Molecular Dynamics* (New York: Wiley) p13

[3] Yu J, Wang S M, Yuan K J and Cong S L 2006 *Chin. Phys.* **15** 1996

[4] Zhou Z Y and Yuan J M 2007 *Chin. Phys.* **16** 0675

[5] Liu L, Niu Y Y, Yuan K J and Cong S L 2007 *Chin. Phys.* **16** 2957

[6] Chen X W, Zeng Z N, Dai J, Li X F, Li R X and Xu Z Z 2008 *Chin. Phys.* B **17** 1826
[7] Fan X J, Li A Y, Tong D M and Liu C P 2008 *Chin. Phys.* B **17** 2522
[8] Zhang S A, Wang Z G and Sun Z R 2008 *Chin. Phys.* B **17** 2914
[9] Han Y C, Yuan K J and Cong S L 2008 *J. Theor. Comput. Chem.* **7** 1159
[10] Han Y C, Yuan K J, Hu W H and Cong S L 2009 *J. Chem. Phys.* **130** 044308
[11] Scherer N F, Carlson R J, Matro A, Du M, Ruggiero A J, Romero-Rochin V, Cina J A, Fleming G R and Rice S A 1991 *J. Chem. Phys.* **95** 1487
[12] Blanchet V, Bouchène M A and Girard B 1998 *J. Chem. Phys.* **108** 4862
[13] Cina J A 2000 *J. Chem. Phys.* **113** 9488
[14] Humble T S and Cina J A 2004 *Phys. Rev. Lett.* **93** 060402
[15] Ohmori K, Sato Y, Nikitin E E and Rice S A 2003 *Phys. Rev. Lett.* **91** 243003
[16] Katsuki H, Chiba H, Girard B, Meier C and Ohmori K 2006 *Science* **311** 1589
[17] Wollenhaupt M, Assion A, Liese D, Sarpe-Tudoran Ch, Baumert T, Zamith S, Bouchene M A, Girard B, Flettner A, Weichmann U and Gerber G 2002 *Phys. Rev. Lett.* **89** 173001
[18] Lindner F, Schätzel M G, Walther H, Baltuška A, Goulielmakis E, Krausz F, Milošević D B, Bauer D, Becker W and Paulus G G 2005 *Phys. Rev. Lett.* **95** 040401
[19] Ishikawa K L 2006 *Phys. Rev.* A **74** 023806
[20] Skovsen E, Machholm M, Ejdrup T, Thøgersen J and Stapelfeldt H 2002 *Phys. Rev. Lett.* **89** 133004
[21] Petersen C, Péronne E, Thøgersen J, Stapelfeldt H and Machholm M 2004 *Phys. Rev.* A **70** 033404
[22] Han Y C, Yuan K J, Hu W H, Yan T M and Cong S L 2008 *J. Chem. Phys.* **128** 134303
[23] Che J, Krause J L, Messina M, Wilson K R and Yan Y 1995 *J. Phys. Chem.* **99** 14949
[24] de Jong W A, Visscher L and Nieuwpoort W C 1997 *J. Chem. Phys.* **107** 9046
[25] Numico R, Keller A and Atabek O 1998 *Phys. Rev.* A **57** 2841
[26] Han Y C, Wang S M, Yuan K J and Cong S L 2007 *Chem. Phys.* **333** 119
[27] Marston C C and Balint-Kurti G G 1989 *J. Chem. Phys.* **91** 3571
[28] Han Y C, Wang S M, Yuan K J and Cong S L 2006 *J. Theor. Comput. Chem.* **5** 743
[29] Feit M D, Fleck J A and Steiger A 1982 *J. Comput. Phys.* **47** 412